LCL Filter Design and Control for Grid-connected PWM Converter

Byung-Geuk Cho[1], Seung-Ki Sul[1], Hyunjae Yoo[2], and Seung-Min Lee[2]

[1] Seoul National University
School of Electrical Engineering & Computer Science #24, ENG-420, Seoul National University Gwanak P.O.BOX34, Seoul, Korea(ZIP 151-744)
bk8089@eepel.snu.ac.kr

[2] SAMSUNG HEAVY INDUSTRIES Co. Ltd. Power & Control Systems Division
493, Banweol-dong, Hwasung-city
Gyeonggi-do, Korea
hyunjae.yoo@samsung.com

***Abstract*-- This paper describes LCL filter design and control for grid-connected PWM converter. To attenuate switching harmonics on grid side with an LCL filter, cost-effectiveness must be considered to select filter parameters. This paper proposes a filter design method based on a computer simulation tool. Depending on user's optimal cost function, filter parameters are chosen without tedious and repetitive mathematical calculations. On the other hand, damping factors must be introduced in control of LCL filter to suppress the inherent resonant characteristics. Since the resonance phenomenon is minimized by increasing the ratio of switching frequency to fundamental grid frequency in most conventional researches, it is difficult to be employed in high power system due to the limited switching frequency of power semiconductors in the converter. In this paper, a novel current controller with generalized gain determination is suggested. Discrete time controller based on only grid voltages and currents information is introduced, which yields desirable dynamic response even in lower switching frequency of PWM converter. Simulations and experimental results are presented to validate the proposed design and control procedures.**

***Index Terms*-- LCL filter design/control, discrete time controller, PWM converter.**

I. INTRODUCTION

PWM voltage source boost converters are increasingly deployed for 3 phase grid connection to regenerative energy sources such as wind power and solar power. In grid-connected PWM converter operation, fulfillment for current harmonic restrictions is one of the critical issues and accordingly L filters or LCL filters are mainly inserted between the grid and converter to reduce harmonic components from PWM switching. Determination of the filter parameter is a crucial design factor to enhance cost-effectiveness of the system. From economical point of view, LCL filters are more attractive because stronger harmonics attenuation is relatively achievable compared to the same size L filters and consequently lower switching frequency is allowable in the case of the same harmonic current limitation.

Several good criteria have been reported to select LCL filter parameters in conventional researches. In [1], filter capacitor is limited to 0.05pu to restrict grid side power factor error derived from simple converter current feedback control and iteratively inductance values have to be adjusted. Bessel function based filter design method has been proposed in [2]. Under the assumption of SPWM/ZSS-PWM, dominant harmonic's ripple is calculated by applying Bessel function. However, for complicated current ripple calculation, LCL filter was modeled as L filter, which is not valid when switching frequency is not far from the resonant frequency.

In this paper, a filter design method based on a computer simulation tool is proposed. The procedure is simple but provides satisfactory filter parameters so that the existing grid standard, e.g IEEE 519-1992, is fulfilled. Depending on user's optimal cost function, filter parameters are selected without tedious and repetitive mathematical calculations.

In terms of current control, damping factors must be included to suppress the inherent resonant characteristics of LCL filters. To implement active damping, converter current feedback control has been commonly used [1]-[3]. This method is robust to the variation of grid impedance and highly stable. However, gain determination requires tuning process and the accuracy of control in grid side power factor is deficient and as a result capacitor value has to be limited in filter design. Analysis on the stability of simple grid/converter side current feedback was conducted and shows limitation for their application [4][5]. Approximation of LCL filter to L filter was attempted in [6] by partially feed-forwarding converter and grid side currents. In this method, power factor error was improved but the system is stable only with high ratio of switching frequency to resonant frequency. In [7], resonant currents, obtained from PQR transformation, are inversely fed into the controller as reference. However, sufficiently wide bandwidth of controller is required to control resonant frequency and also power factor error exists due to the converter current based control.

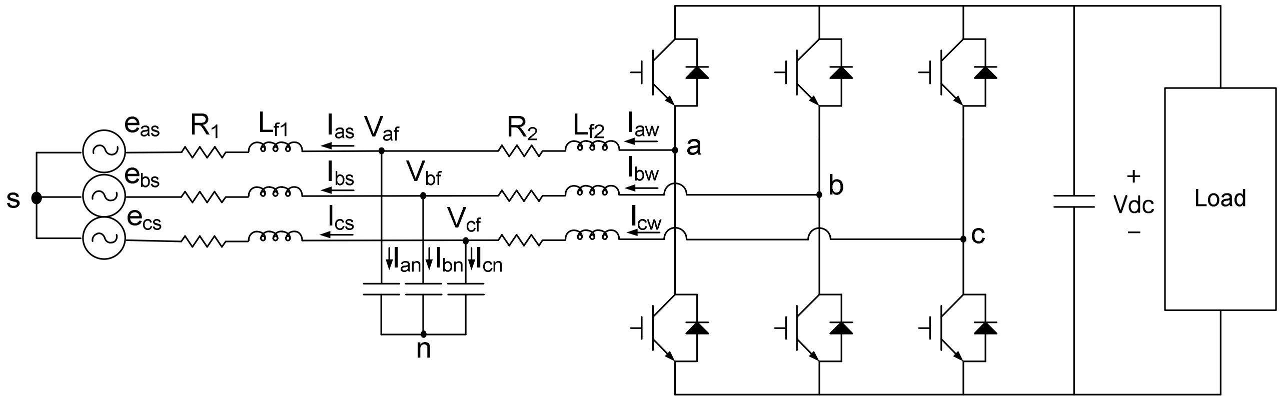

Fig. 1. System configuration with LCL filter of grid-connected PWM converter.

In [8], cascaded current controller was proposed and power factor was precisely controlled because of grid current measurements. Implementation of an observer for other required information makes the system complicated.

In this paper, a novel current controller with generalized gain determination depending on primarily filter parameters is proposed. The complexity of gain calculation is inversely proportional to additional installable sensors in the system. For the lower switching frequency of large capacity PWM converter, discrete time controller with only grid voltages and current information is introduced, which yields desirable dynamic response even in lower switching frequency. No observers or estimators are needed in this approach. Simulations and experimental results are presented to validate the effectiveness of the works

II. LCL FILTER DESIGN

The top priority in filter design is the grid harmonic current standards, such as IEEE 519-1992, IEC 61000-3-2 and IEC 61000-3-4. In this paper, system design to meet the IEEE 519-1992 is the goal and table 1 shows the harmonic current restriction. As the application of LCL filter with PWM converter is power generation equipment, the shadowed line in the table should be met. Among the harmonics presented in table 1, the most significant harmonic components are switching frequency and resonant frequency of the filter. However, as the resonant component is subject to switching frequency and control algorithm, only switching components can be considered in filter design phase.

Variables of the system dealt in this paper are displayed in table 2. Power semiconductor devices and grid capacity are taken into account to decide DC link voltage and power rating. For switching frequency, it is generally designated from 60 to 200 times of fundamental frequency of grid in order to reduce switching ripple and facilitate the design of current controller. However, in this paper, switching frequency is set 2.5 kHz(almost 41st harmonic) to consider application of LCL filter to high power low switching frequency system even though capacity of the system under study is only 3kW considering laboratory test setup.

TABLE 1
Current Distortion Limits for General Distribution Systems
120V through 69000V
IEEE 519-1992

Maximum Harmonic Current Distortion in Percent of I_L

Individual Harmonic Order (Odd Harmonics)

I_{sc}/I_L	< 11	11< h <17	17< h <23	23< h <35	35≤ h	TDD
< 20*	4.0	2.0	1.5	0.6	0.3	5.0
20<50	7.0	3.5	2.5	1.0	0.5	8.0
50<100	10.0	4.5	4.0	1.5	0.7	12.0
100<1000	12.0	5.5	5.0	2.0	1.0	15.0
>1000	15.0	7.0	6.0	2.5	1.4	20.0

Even harmonics are limited to 25% of the odd harmonic limits above.

Current distortions that result in a dc offset, e.g., half-wave converters, are not allowed.

*All power generation equipment is limited to these values of current distortion, regardless of actual I_{sc}/I_L.

Where
I_{SC} = maximum short-circuit current at PCC.
I_L = maximum demand load current (fundamental frequency component) at PCC

TABLE 2
System variables for LCL filter design

Rated power	3 kW
DC link	330 V
Rated line voltage	220Vrms
Rated current	7.873Arms
Grid frequency	60 Hz
Switching frequency	2.5 kHz

Fig. 1 illustrates the system configuration with LCL filter of grid-connected PWM converter. R1 and R2 stand for resistances of grid side inductor and converter side inductor, respectively and (1) ~ (4) represent the mathematical descriptions for the LCL filter.

$$V_{abcn} = R_2 i_{abcw} + L_{f2}\frac{di_{abcw}}{dt} + V_{abcfn} \quad (1)$$

$$V_{abcfn} = R_1 i_{abcs} + L_{f1}\frac{di_{abcs}}{dt} + e_{abcs} \quad (2)$$

$$i_{abcn} = C_f \frac{di_{abcn}}{dt} \quad (3)$$

$$i_{abcw} = i_{abcn} + i_{abcs} \quad (4)$$

Based on the above equations, Bode plot of grid side current to filter input voltage is displayed in Fig. 2 and it is noticeable that if resonant frequency component is contained in the converter output voltage, then the grid current would diverge or include undesirable harmonics.

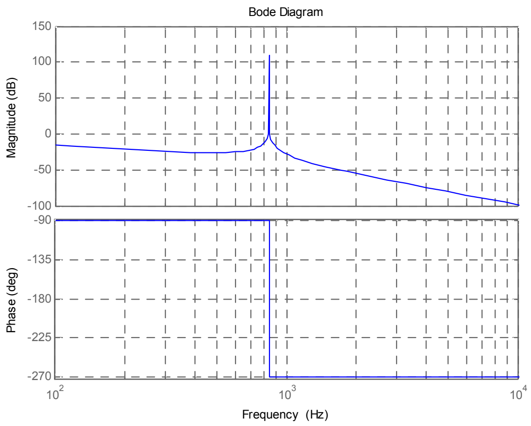

Fig. 2. Bode plot of grid current to LCL filter input voltage

The resonant frequency is normally chosen over 10 times of grid frequency not to be excited by grid frequency. Since various filter parameters can be considered according to the designed resonant frequency, resonant frequency is also a critical input factor for the filter design. If the PWM converter input reference voltage is pure sinusoidal and switching frequency is odd-multiple of grid frequency, it is advantageous to set resonant frequency even-multiple of grid frequency in terms of interaction between switching frequency and resonant frequency because PWM harmonics mostly exist in odd-multiples [2].

With the fixed resonant frequency, numerous combinations for filter parameters are possible. To sort out the combinations, unit step changes are made in the per unit values of capacitor and converter side inductor at the fixed resonant frequency. Then the grid side inductance is derived from the resonant frequency equation and finally ideal filter input voltage for unit power factor in the grid side can be computed. To figure out switching component in the current, PWM block is incorporated and FFT analysis is executed. If IEEE 519-1992 standard is satisfied for all frequencies, the filter parameters are stored and next parameter combinations are examined. Fig. 3 demonstrates the flow chart of proposed design process step by step and table 3 presents several sampled combinations of filter parameters.

TABLE 3
Sampled combination for different resonant frequency

Resonant frequency	Parameters		
	L_{f1}(pu)	L_{f2}(pu)	C_f(pu)
840[Hz]	0.1083	0.119	0.09
	0.0771	0.151	0.1
960[Hz]	0.021	0.287	0.2
	0.163	0.15	0.05
1080[Hz]	0.2017	0.21	0.03
	0.1017	0.32	0.04

There is no specific rule in classifying the diverse parameter combinations obtained from the simulation. It is definitely dependent on user's cost function. For example, optimal selection can be made to have either the minimum expense by imposing different price scaling coefficient on capacitor and inductors or the least capacitor combination to produce less power factor error

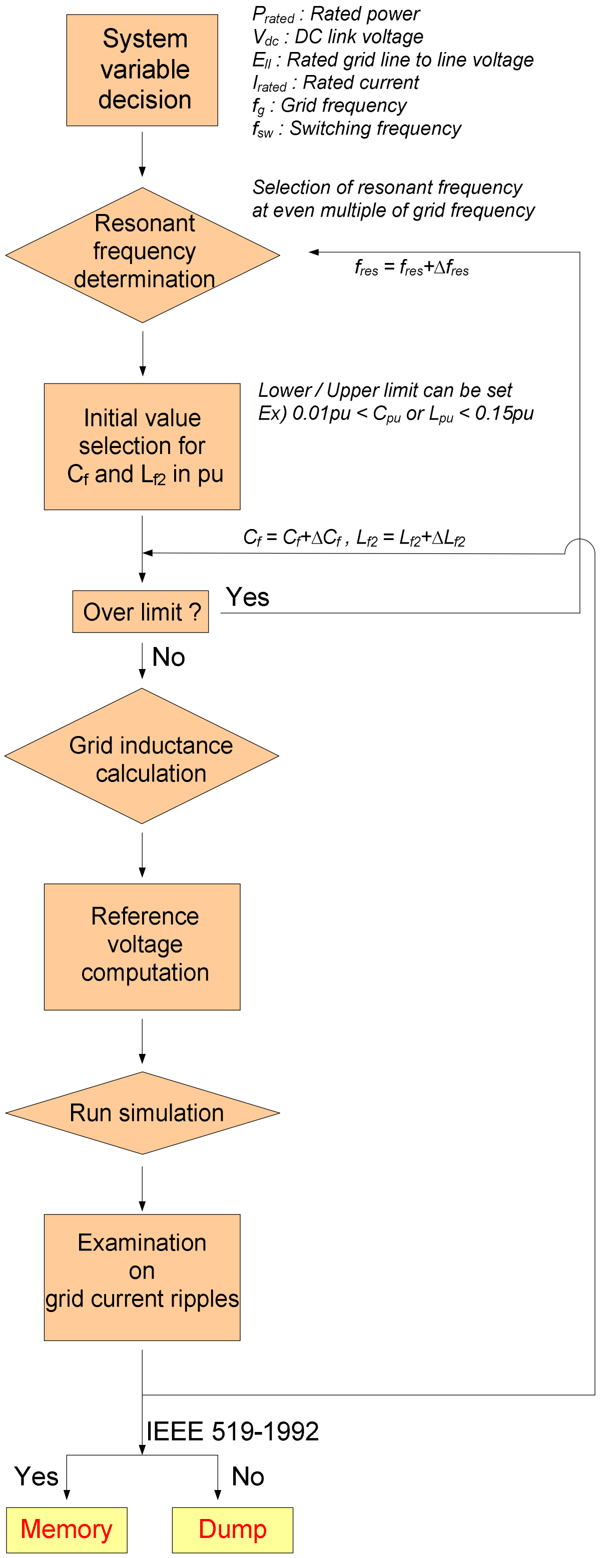

Fig. 3. Flow chart of proposed LCL filter design method

for simple converter current feedback control. Consequently, the proposed filter design method provides a lot of different filter options for different users.

III. LCL FILTER CONTROL

In this paper, novel current controllers are proposed depending on system conditions, e.g switching frequency. Gains are determined by only filter parameters and desirable dynamic response. For the design of controllers, PWM converter with LCL filter is described as (5) ~ (9) in reference frame synchronized to positive q-axis of grid voltage. In terms of time base, a continuous time controller is acceptable when sufficiently high switching frequency is guaranteed. However, a discrete time controller has to be implemented to secure stability of the system where switching frequency is limited. Continuous time controller design is followed by discrete time controller design.

$$V_{dqn}^{r} = R_2 i_{dqw}^{r} + L_{f2}\frac{di_{dqw}^{r}}{dt} + j\omega_r L_{f2} i_{dqw}^{r} + V_{dqfn}^{r} \tag{5}$$

$$V_{dqfn}^{r} = R_1 i_{dqs}^{r} + L_{f1}\frac{di_{dqs}^{r}}{dt} + j\omega_r L_{f1} i_{dqs}^{r} + e_{dqs}^{r} \tag{6}$$

$$i_{dqn}^{r} = C_f\frac{di_{dqn}^{r}}{dt} + j\omega_r C_f V_{dqfn}^{r} \tag{7}$$

$$i_{dqw}^{r} = i_{dqs}^{r} + i_{dqn}^{r} \tag{8}$$

$$e_{ds}^{r} = 0,\; e_{qs}^{r} = E \tag{9}$$

where,

ω_r : grid frequency[rad/s]

E : Peak value of grid phase voltage[V].

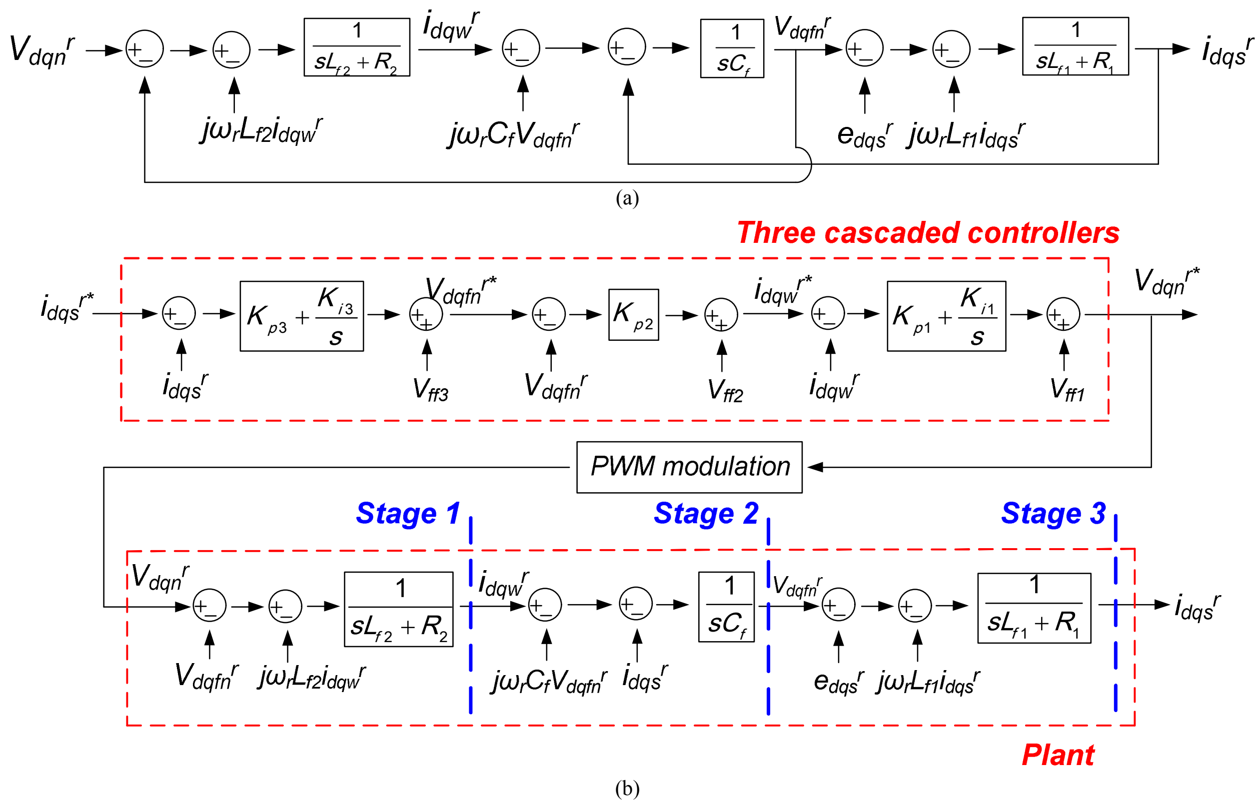

Fig. 4. (a) LCL filter model in synchronous reference frame. (b) Proposed three cascaded current controller

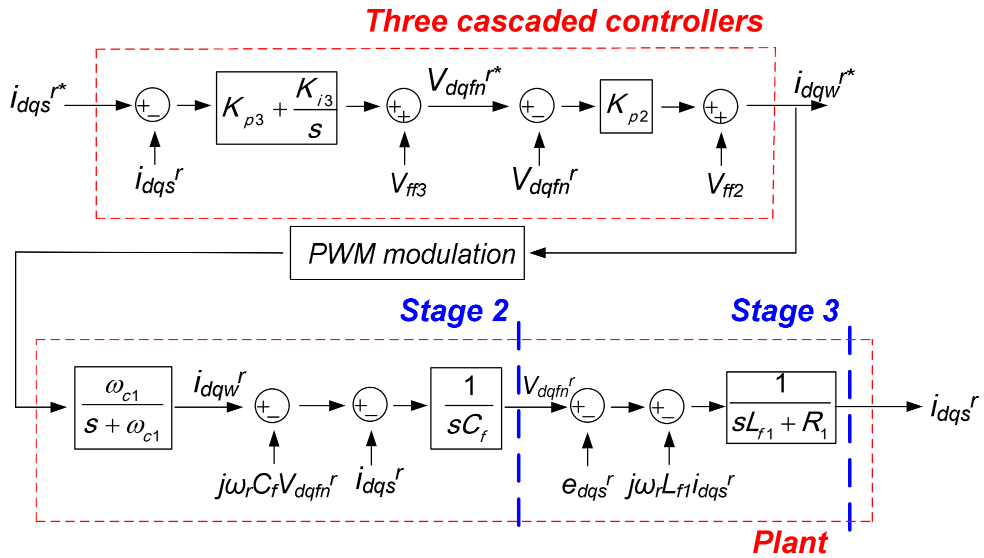

Fig. 5. Equivalent block from the second controller point of view.

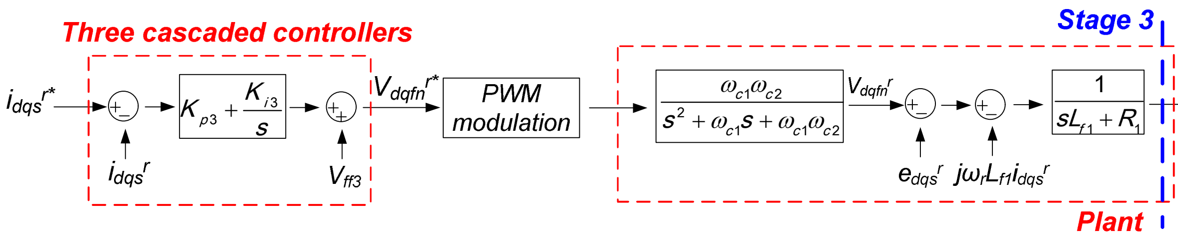

Fig. 6. Equivalent block from the third controller point of view.

A. Continuous time controller design –Multi loop cascaded controller

Fig. 4 displays LCL filter modeling block obtained from the equations (5) ~ (9) and three cascaded current controllers for grid current regulation. If the controller is constructed with the same order as that of the plant, desirable control performance is achievable with very simple gain setup under the assumption that feed-forwarding for the terms outside the closed loop are correct. To cancel out the poles in plant by zeros of the controller, gains of each controller can be simply determined as in (10). Then, with accurate feed-forwarding compensation, the overall closed loop transfer function becomes third order low pass filter format as in (11). For successful realization of this controller, precise feed-forwarding is significantly critical and the values are decided as following.

1) V_{ff1} : Being connected to the stage 1 directly, V_{ff1} is simply decided as in (12).
2) V_{ff2} : If V_{ff1} is accurate, the closed loop in Fig. 4(b) can be equivalently converted to Fig. 5 from the second controller point of view because the inner loop is described as a first order low pass filter. Therefore, V_{ff2} is given as in (13) and the derivative terms can be acquired from equations (5) ~ (9) without derivative calculation.
3) V_{ff3} : Similarly, if V_{ff1} and V_{ff2} are accurate, the closed loop in Fig. 4(b) can be equivalently converted to Fig. 6 from the third controller point of view because the inner loop is described as a second order low pass filter. Therefore, V_{ff3} is given as in (14) and derivative terms can be acquired from equations (5) ~ (9) without derivative calculation.

$$K_{p1} = L_{f2}\omega_{c1}, K_{i1} = R_2\omega_{c1} \tag{10-a}$$
$$K_{p2} = C_f\omega_{c2} \tag{10-b}$$
$$K_{p3} = L_{f1}\omega_{c3}, K_{i3} = R_1\omega_{c3} \tag{10-c}$$

$$\frac{i^r_{dqs}}{i^{r*}_{dqs}} = \frac{\omega_{c1}\omega_{c2}\omega_{c3}}{s^3+\omega_{c1}s^2+\omega_{c1}\omega_{c2}s+\omega_{c1}\omega_{c2}\omega_{c3}} \tag{11}$$

$$V_{ff1} = V^r_{dqfn} + j\omega_r L_{f2} i^r_{dqw} \tag{12}$$
$$V_{ff2} = \frac{s+\omega_{c1}}{s}\left(i^r_{dqs} + j\omega_r C_f V^r_{dqfn}\right) \tag{13}$$
$$V_{ff3} = \frac{s^2+\omega_{c1}s+\omega_{c1}\omega_{c2}}{\omega_{c1}\omega_{c2}}\left(e^r_{dqs} + j\omega_r L_{f1} i^r_{dqs}\right) \tag{14}$$

Simulation results are presented in Fig. 7 to evaluate the cascaded controller. Expected outputs stand for the required response according to equation (11). As indicated, proposed cascaded controller shows the exactly same dynamic response as desired in continuous time domain. However, due to the digital delay and deficient feed-forward compensation for derivative terms, digital implementation leads to deviation from the desired response. Therefore, while this method provides very simple way of gain determination, it is realizable mostly under the condition with high enough switching frequency of converter and additional sensors for accurate feed-forwarding.

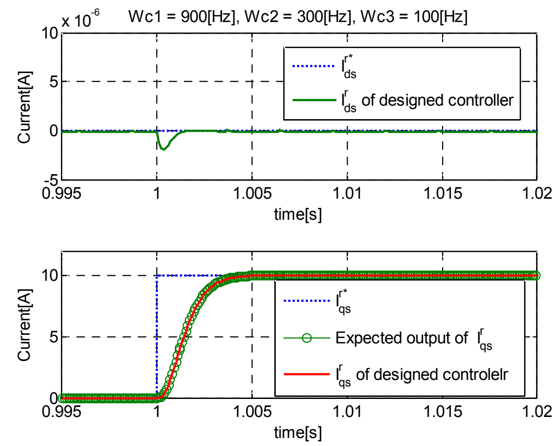

(a) Current control performance in continuous time realization without PWM

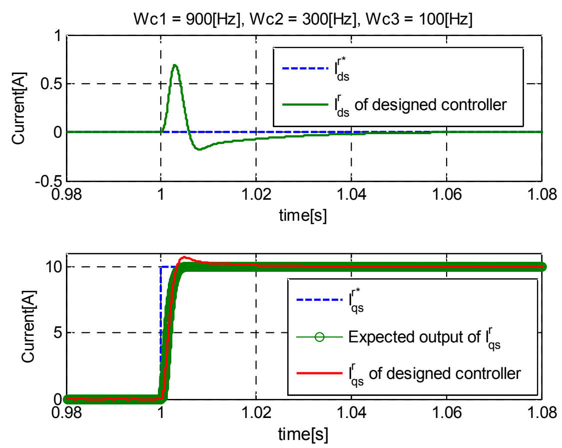

(b) Current control performance in digital realization with PWM (fsw = 10kHz)

Fig. 7 Simulation results of cascaded controller (Lf1=0.1083pu, Lf2=0.119pu, Cf=0.09pu, fres = 840Hz)

B. Continuous time controller design – Single loop complex controller

To cope with the problem of additional sensors in the cascaded controller, single loop current controller is suggested. (15) is rearranged form of LCL filter with only grid currents/voltages and adjusted equivalent model is depicted in Fig. 8. To prevent additional sensors, feed-forwarding compensation must be realized with only grid currents or voltages. Therefore, single loop complex current controller must be designed by including coupling terms in closed loop because derivatives of grid current require information of other components.

$$V_{dqn}^r = (A_1 s^3 + B_1 s^2 + C_1 s + D_1) i_{dqs}^r + j(E_1 s^2 + F_1 s + G_1) i_{dqs}^r + (1 - \omega_r^2 C_f L_{f2}) e_{dqs}^r + j\omega_r C_f R_2 e_{dqs}^r \tag{15}$$

where,

$A_1 = C_f L_{f1} L_{f2}, B_1 = C_f(L_{f1} R_2 + L_{f2} R_1),$
$C_1 = L_{f1} + L_{f2} + C_f R_1 R_2 - 3\omega_r^2 C_f L_{f1} L_{f2},$
$D_1 = R_1 + R_2 - \omega_r^2 C_f(L_{f1} R_2 + L_{f2} R_1),$
$E_1 = 3\omega_r C_f L_{f1} L_{f2}, F_1 = 2\omega_r C_f(L_{f1} R_2 + L_{f2} R_1),$
$G_1 = \omega_r(L_{f1} + L_{f2} + C_f R_1 R_2 - \omega_r^2 C_f L_{f1} L_{f2})$

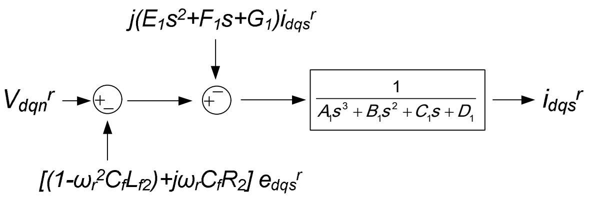

Fig. 8 Adjusted single loop model of LCL filter

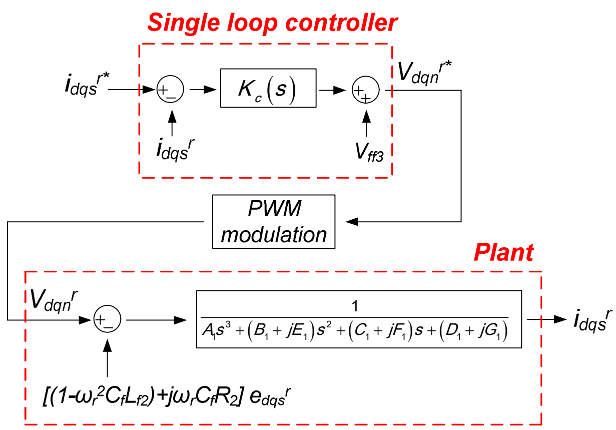

Fig. 9 Structure of continuous time single loop controller

Fig. 9 depicts the structure of single loop controller. For 3rd order low pass filter characteristics, feed-forward terms and gains are chosen as in (16) and (17), respectively.

$$V_{ff} = \left[(1 - \omega_r^2 C_f L_{f2}) + j\omega_r C_f R_2\right] e_{dqs}^r \tag{16}$$

$$K_c(s) = \omega_{c1}\omega_{c2}\omega_{c3}\left[\left(\frac{A_1 s^3 + B_1 s^2 + C_1 s + D_1}{s^3 + \omega_{c1} s^2 + \omega_{c1}\omega_{c2} s}\right) + j\frac{E_1 s^2 + F_1 s + G_1}{s^3 + \omega_{c1} s^2 + \omega_{c1}\omega_{c2} s}\right] \tag{17}$$

Simulation result with different filter parameters from those of cascaded controller is shown in Fig. 10. Even though resonant frequency increases, grid current is effectively controlled with lower switching frequency. For digital implementation, 3rd order function $K_c(s)$ is realized by forward Euler method.

Reasons for better performance by the single loop controller can be analyzed with frequency response. The cascaded controller hires three series PI controllers, which have infinite gain at DC component as shown in Fig. 11. If errors from deficient feed-forwarding occur, high frequency components are included in the closed loop and the innermost PI controller with the maximum gain would attempt to regulate harmonics. Then, since PI controller shows almost constant gain over certain frequency, other frequency components such as resonant elements are contained in the output of the PI controller. However, if switching frequency is limited, accurate output synthesis is impossible and it leads to unstable states. To prevent this, if gains are set low, the outer most controller's gain becomes also small and DC component control is threatened. Therefore, cascaded controller shows stable operation when enough high switching frequency is guaranteed with appropriate gains setup at the expense of simple gain determination. On the other hand, as single loop controller has negative infinite gain at resonant frequency under Nyquist frequency but positive gain for lower frequencies as shown in Fig. 12, relatively better performance is achievable.

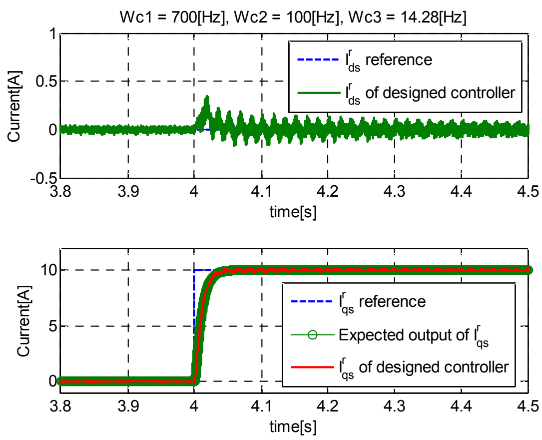

Fig. 10 Simulation results of continuous time single loop controller (Lf1=0.2017pu, Lf2=0.21pu, Cf=0.03pu, fres = 1.08kHz,fsw = 2.5kHz)

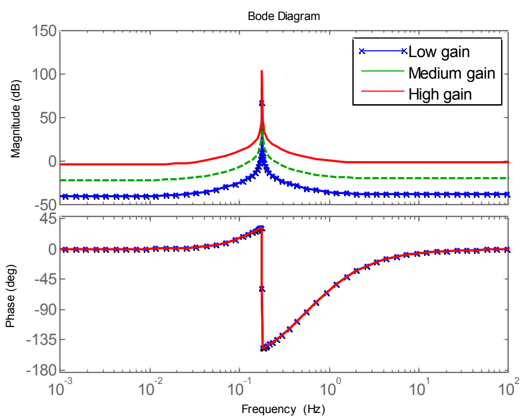

Fig. 11 Bode plot of PI controller in cascaded controller

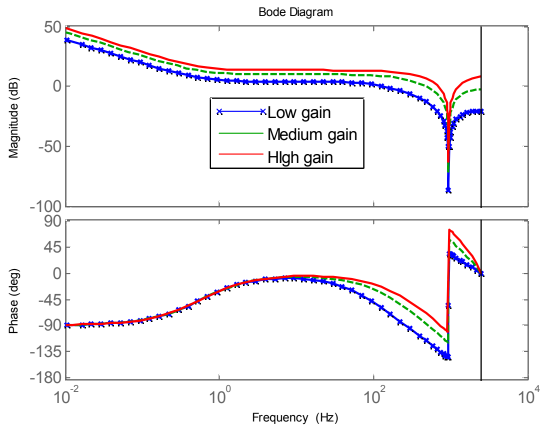

Fig. 12 Bode plot of single loop controller

C. Discrete time controller design – Single loop complex controller

To improve stability of continuous single loop controller in digital control, plant is modeled in discrete time domain by using ZOH(Zero Order Hold) [9]. Z-domain modeling is displayed in Fig. 13 and comparison between continuous time model and z-domain model is made in Fig. 14 based on (18).

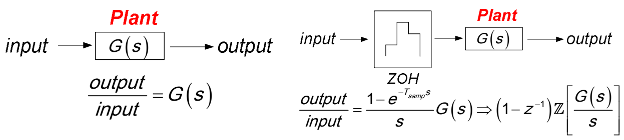

(a) Continuous (b) Discrete

Fig. 13 Z-transformation

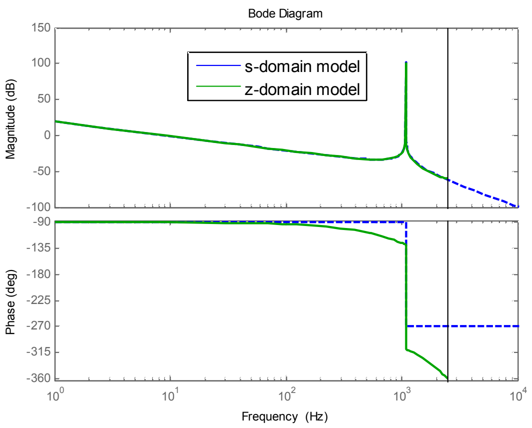

Fig. 14 Comparison of transformed discrete model with continuous model in frequency domain

$$\frac{i_{abcs}}{V_{abcn}} = \frac{1}{s^3 C_f L_{f1} L_{f2} + s(L_{f1} + L_{f2})}$$
$$\gg \frac{z-1}{z}\left[\frac{1}{B}\frac{T_{sam\,p} z}{z^2-2z+1} - \frac{\sqrt{A}}{B\sqrt{B}}\frac{z\sin\left(\sqrt{\frac{B}{A}}T_{sam\,p}\right)}{z^2-2z\cos\left(\sqrt{\frac{B}{A}}T_{sam\,p}\right)+1}\right] \quad (18)$$

where,

$A = C_f L_{f1} L_{f2}, B = L_{f1} + L_{f2}$

IV. Experiment

Experiment has been conducted by discrete time controller. Table 4 shows specifications for the experimental condition. To evaluate current control performance, DC link voltage is supplied by constant DC power source and smaller grid voltage is used due to different filter parameters from the designed values. However, constant magnitude grid voltage has no effect on the current control performance unless faulty or distorted grid conditions must be considered.

Fig. 15 presents q-axis response to step reference change. Fig. 16 shows corresponding grid phase current and voltage. As proved, grid current follows successfully the desired trace. The ripples seen in synchronous reference frame is 2^{nd} order harmonics resulted from filter inductance unbalance. Balanced AC power source have been connected to confirm and current waveforms are demonstrated in Fig. 17.

TABLE 4
Specifications for experiment

DC link	310[V]	Lf1	13.3[mH]
Rated line Voltage/frequency	170[Vrms]/60[Hz]	Lf2	14[mH]
Rated current	8[Arms]	Cf	13[uF]
Switching	2.5[kHz]	Resonance	534[Hz]

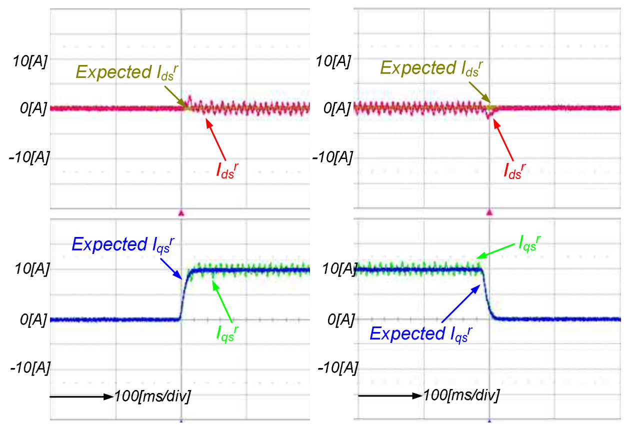

Fig. 15 Positive/Negative step response of discrete time controller

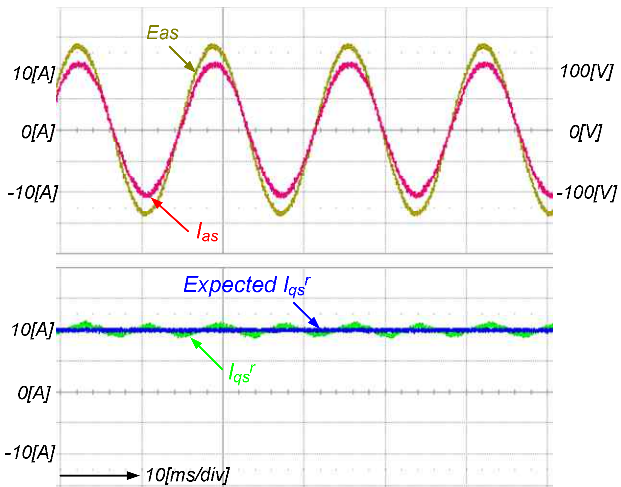

Fig. 16 Positive/Negative step response of discrete time controller

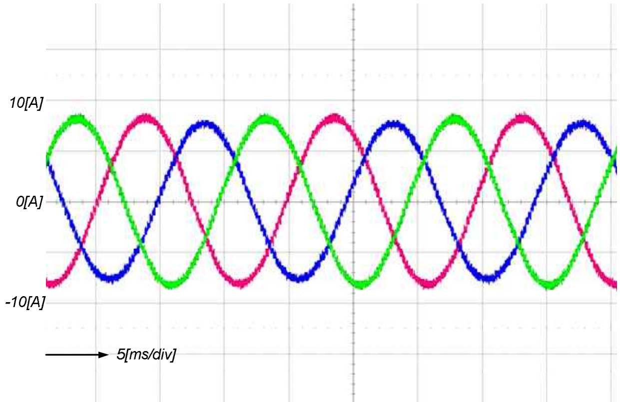

Fig. 17 Current unbalance from inductance unbalance

V. Conclusions

LCL filter design and control has been described for harmonic attenuation of grid-connected PWM converter. Since there is no specific rule for filter design and criteria are various depending on user' requirement or application environment, the approach is ambiguous. This paper proposes a new design method to find diverse filter parameter combinations based on computer simulation tool. The proposed design method is independent of control issue in terms of switching ripples and different values are available for different users.

Three control methods for designed LCL filter are also suggested. One of the most significant point in all three controllers is that no tuning process is required and gains are automatically determined by filter parameters and system variables such as switching frequency. Cascaded controller is limited in application but gain setup is relatively easy. Single loop controllers exhibits satisfactory performance under low ratio of switching frequency to grid fundamental frequency. Simulations and experimental results complement the works.

Acknowledgment

This work has been supported by Samsung Heavy Industries.

References

[1] M. Liserre, F. Blaabjerg, and S. Hansen, "Design and control of an LCL-filter based three phase active rectifier," IEEE Trans. Industry Applications, vol. 41, pp. 1281-1291, 2005.

[2] K. Jalili and S. Bernet, "Design of LCL Filters of Active-Front-End Two-Level Voltage-Source Converters," IEEE Trans. Industrial Electronics, vol. 56, pp. 1674-1689, 2009.

[3] M. Malinowski and S. Bernet, "A Simple Voltage Sensorless Active Damping Scheme for Three-Phase PWM Converters With an LCL Filter," IEEE Trans. Industrial Electronics, vol. 55, pp. 1876-1880, 2008.

[4] J. Dannehl, F.W. Fuchs, S. Hansen and P.B. Thogersen, "Investigation of Active Damping Approaches for PI-based Current Control of Grid-connected Pulse Width Modulation Converters With LCL Filters," IEEE Trans. Industrial Applications, vol. 46, pp. 1509-1517, 2010.

[5] J. Dannehl, C. Wessels and F.W. Fuchs, "Limitations of Voltage-Oriented PI Current Control of Grid-Connected PWM Rectifiers With LCL Filters," IEEE Trans. Industrial Electronics. vol. 56, pp. 380-388, 2009.

[6] Guoqiao Shen, Xuancai Zhu, Jun Zhang and Dehong Xu, "A New Feedback Method for PR Current Control of LCL Filter Based Grid Connected Inverter," IEEE Trans. Industrial Electronics. vol 57, pp.2033-2041, 2010.

[7] Hea-Gwang Jeong, Kyo-Beum Lee, Sewan Choi and Woojin Choi, "Performance Improvement of LCL Filter Based Grid Connected Inverters Using PQR Power Transformation," IEEE Trans. Power Electronics. vol 25, pp.1320-1330, 2010.

[8] E.J. Bueo, F. Espinosa, F.J. Rodriguez, J. Urefia and S. Cobreces, "Current control of voltage source converters connected to the grid through an LCL-filter," Power Electronics Specialists Conference, 2004. Vol 1, pp.68-73.

[9] "Discrete Time Control System," – Katsuhiki Ogata, Prentice-Hall